HAL
open science

Fast evolving spatial structure of auroral parallel electric fields

Vincent Génot, P. Louarn, F. Mottez

To cite this version:

Vincent Génot, P. Louarn, F. Mottez. Fast evolving spatial structure of auroral parallel electric fields. Journal of Geophysical Research, 2001, 106, pp.29633-29644. 10.1029/2001JA000076 . hal-00290080

HAL Id: hal-00290080

https://hal.science/hal-00290080v1

Submitted on 25 Jun 2008

HAL is a multi-disciplinary open access archive for the deposit and dissemination of scientific research documents, whether they are published or not. The documents may come from teaching and research institutions in France or abroad, or from public or private research centers.

L'archive ouverte pluridisciplinaire **HAL**, est destinée au dépôt et à la diffusion de documents scientifiques de niveau recherche, publiés ou non, émanant des établissements d'enseignement et de recherche français ou étrangers, des laboratoires publics ou privés.

Fast evolving spatial structuration of auroral parallel electric fields

V. Génot
Astronomy Unit, Queen Mary, University of London, London, United Kingdom

P. Louarn
Centre d'Etude Spatiale des Rayonnements, Toulouse, France

F. Mottez
Centre d'étude des Environnements Terrestre et Planétaires, Vélizy, France

Short title: STRUCTURATION OF THE PARALLEL ELECTRIC FIELD

Abstract.

We use a fully non linear PIC gyrocinetic code to investigate the role of Alfvén waves in the auroral particle acceleration. The propagation of an Alfvén wave in an inhomogeneous auroral plasma, described by a density cavity, is considered. Parallel electric fields are generated on the edges of the cavity leading to an efficient electron acceleration and to the formation of electron beams. A beam/plasma instability takes place. It evolves nonlinearly and small scale electrostatic structures are created and propagate at velocity close to the Alfvén velocity. A first category of these structures could be assimilated to weak double layers, whereas a second may be related to electron phase space holes. This study demonstrates the potential importance of Alfvén waves in the auroral acceleration and the coupling between large-scale electromagnetic and small-scale electrostatic phenomena.

1. Introduction

The auroral particle acceleration results from a still not fully described chain of processes. In short, the problem is to understand how incoming energy from distant regions of the magnetosphere can be efficiently converted into the kinetic energy of accelerated particles, up to KeV energies, in regions of limited extension (a few 1000 km in the parallel to the magnetic field direction, a few 10 km in the perpendicular one). In principle, the existence of parallel electric fields would be the simplest and the most efficient way to accelerate particles. However, the large parallel conductivity that characterizes the auroral plasma is expected to immediately short-circuit such fields. The main difficulty of the problem of the auroral acceleration is thus to understand how parallel electric fields can form and be maintained in collisionless plasmas and to identify their typical spatial and temporal scales.

A number of theoretical models can be invoked for explaining the existence of parallel electric fields. For example, microscopic processes may (i) introduce anomalous resistivity along the auroral magnetic field lines, [*Papadopoulos,* 1977], (ii) create small-scale non linear structures [*Temerin et al.,* 1982; *Boström et al.,* 1988; *Mälkki et al.,* 1993; *Mottez et al.,* 1992; *Mangeney et al.,* 1999], or (iii) directly transfer energy from high frequency waves [*Bingham et al.,* 1984]. On larger scales, global ionosphere/magnetosphere electrostatic potential difference can also develop over the whole auroral field lines (as in the strong double-layer model [*Miura and Sato,* 1980] or in the kinetic model initially proposed by [*Alfvén and Fälthammar,* 1963], see also [*Chiu and Schulz,* 1978]). By contrast with these static models, other ones take into account the dynamical nature of the auroral phenomena. For example, in the kinetic/inertial Alfvén wave model [*Hasegawa,* 1976], the parallel electric field results from an electron inertia effect that modify the dispersion of shear Alfvén waves in very oblique propagation (typically $k_\perp c/\omega_{pe} \sim 1$).

It must be recognized that these different models are not concurrent. Most of

their ingredients are indeed actually observed by spacecraft in the auroral regions. For example, observations by FREJA [*Louarn et al.,* 1994; *Wahlund et al.,* 1994; *Seyler et al.,* 1995; *Volwerk et al.,* 1996; *Stasiewicz et al.,* 1998; *Knudsen,* 1996; *Chust et al.,* 1998] clearly suggest that the low frequency electromagnetic fluctuations play an important role in the auroral energization processes (see also FAST observations, for instance [*Chaston et al.,* 1999]). On the other hand, various types of small scale non-linear structures have been identified in the auroral plasmas. From the VIKING and the FREJA wave experiments (see references above and [*Berthomier et al.,* 1998]), solitary structures of small amplitude (potential fluctuations of a few V), sometimes presenting a net potential difference between their two sides, have been observed in regions of moderate acceleration (regions where the particle energy remains typically below 1 keV). More recently, the existence of intense electrostatic structures has been reported from FAST observations [*Ergun et al.,* 1998a; *Ergun et al.,* 1998b] in regions of return currents between 2000 and 4000 km. The amplitude of their electric fields reaches 2.5 V/m over parallel size of a few Debye lengths. They have been described as phase-space electron holes by [*Muschietti et al.,* 1999].

Given the complexity of the situation, an important question is to understand how the two types of models (the Alfvén wave model and the ones invoking the formation of small scale electrostatic structures) could be connected. This point is absolutely not discussed in studies of the Alfvén wave propagation in auroral plasma that are restricted to the linear theory (as in [*Goertz and Boswell,* 1979; *Kletzing,* 1994; *Streltsov and Lotko,* 1995; *Streltsov,* 1999; *Génot et al.,* 1999]). Other studies have idealized the interaction with small scale processes by a simplified form of the anomalous resistivity [*Lysak and Dum,* 1983; *Lysak,* 1990; *Lysak & Lotko,* 1996]. If such an approach can give some of the pertinent scales of the Alfvén wave absorption, it is obviously not adapted to the detailed analysis of their nonlinear evolution. More recently, this point has been specifically studied by bi-fluid models [*Chmyrev et al.,* 1989; *Bellan and Stasiewicz,*

1998; *Seyler,* 1990; *Seyler and Wahlund,* 1996; *Clark and Seyler,* 1999]. They are nevertheless unable to describe precisely the small scale kinetic processes and to predict the effect of the energy dissipation on the particle distribution functions.

On the other hand, numerical simulation describing the formation of small scale electrostatic structures have been performed in idealized situations only. In most cases, they have been restricted to the study of the linear and the nonlinear evolutions of particle beams initially injected in the simulation box [*Omura et al.,* 1996; *Mottez et al.,* 1997; *Goldman et al.,* 1999; *Miyake et al.,* 2000]. A more complex model was recently studied by [*Mandrake et al.,* 2000] who included an inhomogeneity parallel to the magnetic field (action of gravitational attraction). However, this model remains electrostatic which precludes the study of the Alfvén wave propagation.

This is precisely the possible relation between the Alfvén wave propagation and the formation of small scale electrostatic structures that is studied in the present paper. We will use the model presented in [*Génot et al.,* 2000] and will consider the propagation of Alfvén waves in plasma density cavities similar to those actually observed in the auroral acceleration region. As shown with a linear model [*Génot et al.,* 1999], the propagation of an Alfvén wave on the density gradients that characterize the edges of such cavities indeed leads (1) to the rapid formation of small length scales of the order of c/ω_{pe} (inertial regime for the Alfvén wave) and (2) to the development of large scale parallel electric fields that may efficiently accelerate particles. In [*Génot et al.,* 2000], we have used a new gyrocinetic 2.5-D electromagnetic Particle In Cell (PIC) code, specially designed for the study of the low frequency propagation, for quantifying the energy exchange between the Alfvén wave and the particles. From this fully non linear code, it was possible to show that an efficient electron acceleration takes place since typically 10% of the electromagnetic energy is transferred to this population [*Génot et al.,* 2001].

Recent technical improvements give the possibility to extend the regime of parameters of the simulation. Larger simulation boxes can be used and the total

duration of the simulation can be increased. It thus becomes possible to simulate realistic situations characterized by smoother density gradients that lead to a less rapid energy dissipation. The non linear development of the process then becomes more simple to follow. After a brief presentation of the code and the simulation model (section 2), we will describe the initial linear evolution of the system (section 3). The non-linear evolution is studied in section 4, before the conclusion (section 5).

2. Simulation code and model

We use an electromagnetic PIC code that allows to follow the full non-linear and kinetic evolution of the system. The model has two spatial dimensions (x, z) and takes into account the three components of the vector fields (velocities, electromagnetic fields, currents). One of the important characteristics of our numerical code is to use a gyrocinetic description of the electron dynamics. The main advantage of this technique is to save a considerable computing time when simulating low frequency phenomena in highly magnetized plasmas. The time step of the simulation can indeed be larger than the electron gyroperiod without incidence on the validity of the results if the phenomena have characteristic scales longer than the electron gyroperiod. Such a code is thus particularly well adapted to the study of the propagation of low frequency and long wavelength phenomena over a few Alfvén wave periods. It is described in details in [*Mottez et al.,* 1998; *Génot et al.,* 2000].

In order to make the size of our system and computing time acceptable, we had to settle a reduced ion to electron mass ratio $m_i/m_e = 100$. The time, the velocity, the mass, and the charge are respectively normalized to ω_{pe}^{-1},c, m_e, and e (e is the charge of an electron). The ambient magnetic field amplitude is given by the value of the ratio ω_{ce}/ω_{pe}. The electric field is normalized to $\omega_{pe} c m_e/e$.

The initial conditions are analogous to those described in [*Génot et al.,* 2000] and are sketched on Figure 1. Our goal is to study the propagation of an Alfvén wave in

a short scale density depletion (a few 10 km in the perpendicular direction) similar to those actually observed in the auroral region. The density depletion $n_0(x)$ extends all along the direction of the ambient magnetic field ($B_0 = B_{0z}$). z is thus the direction of the static field and also of homogeneity. Periodic boundary conditions are used in both the x and z directions. Along x, one may distinguish five regions: on the two sides of the simulation box, two regions of large density (n_0); in the middle, a density channel (typically $n_0/3$); in between, two regions where the density linearly varies. These two regions of density gradient will play an essential role in the formation of the parallel electric field. The characteristic length of the gradient is larger than the ion Larmor radius: $L_x > \rho_i$. The stability of this density profile has been tested by running a simulation with this initial condition on several hundreds time steps without noticing any sign of evolution.

Compared to the simulations presented in [*Génot et al.,* 2000], the simulation domain is larger (2048×64 instead of 2048×32) and the density gradient is (five times) smaller. For similar amplitudes of the Alfvén wave, smaller parallel electric fields are thus expected. The size of the cells is 1 Debye length (λ_D). Given the temperature of the electron population (~5 keV in the simulation), this corresponds to a spatial scale of ~0.53 km in reality (for a density of 1 cm^{-3}). The total simulation box thus represents 1090×34 km^2 of auroral plasma. This obviously correspond to a rather short portion of the auroral field lines. Nevertheless, this is sufficient to simulate properly the propagation of Alfvén waves. The wavelength, equal to the size of the box, is indeed sufficiently long to restrict the propagation to a domain of small k, where the Alfvén wave dispersion is small. The plasma $\beta = 4\frac{m_e}{m_i}\left(\frac{v_{the}}{v_A}\right)^2$ is 0.0025 and the total number of particles is ~4.5×10^6.

To the cavity, we superimpose a low-frequency wave (Alfvén and/or fast magnetosonic modes) that propagates in the direction of increasing z (from left to right in all the figures) along the ambient magnetic field ($k = k_z$). The initial parallel electric

field is null ($E_z = 0$). To get a linear polarisation (perpendicular electric field in the x direction), LH and RH polarized waves of equal amplitudes have been superposed. The amplitude of the wave is given by the ratio $\delta B/B_0$ of the magnetic field perturbation over the ambient magnetic field. For the simulations presented below, this ratio is 0.05. This is a rather large value compared to what is actually observed (the observed ratio is rather 0.01). This is however mandatory to overtake the noise level and obtain observable effects.

3. Initial linear evolution of the Alfvén Wave on the density gradient

The first part of the simulation, from t=0 to t=400 is consistent with the analysis previously conducted in [*Génot et al.,* 2000]. In Figures 2 and 3, we present the parallel electric field and the electron distribution at t=160 and t=320, respectively.

The uppermost panel is a map of the parallel electric field. To remove a part of the noise generated during the simulation (this is a classical problem of PIC simulations since a limited number of macro-particles is used), the original data set has been filtered by applying a simple sliding average over 40 cells in the z direction. On the same panel, contour plots indicate the position of the density gradients. The gradients are distorted along the parallel direction due to the action of the y electric field component of the waves which generates a global plasma drift velocity $v_{dx} = E_y/B_{0z}$. In the very large wavelength limit ($k \to 0$), E_y vanishes as it is the superposition of Alfvén and magnetosonic components, opposite to each other. In the simulation, the finite value of k leads to different dispersion relations for the two modes and finally to $E_y \neq 0$. This results in a periodic evolution of the shape of the density channel which can be seen on Figures 2, 3, 4 and 6. However, this effect is strongly exaggerated in the figures as the boxes are in fact very elongated in the z direction.

One observes the progressive formation of the parallel field at or close to the density gradients. As discussed in [*Génot et al.,* 1999] and [*Génot et al.,* 2000], the formation of this parallel electric field is linked to the difference between the ion and the electron polarization drifts. This drift results from the propagation of the Alfvén wave or, more precisely, from the time evolution of the perpendicular electric field (the polarization drift is given by $j_x = \frac{mn}{B^2}\frac{\partial E_x}{\partial t}$). The differential drift between the ions and the electrons creates a space charge in or near the density gradients. In the low β plasma that characterizes the auroral region and the simulation, the parallel dynamics of the electrons is the most efficient process for restoring the quasi-neutrality. This explains the formation of a non negligible electric field along the magnetic field lines. At t=320, if one considers the isocontour labelled 0.6 (this isocontour approximately corresponds to a magnetic field line) typical values of 0.002 are reached by the parallel electric over distances ($80c/\omega_{pe}$) of the order of half of the wavelength. Such values correspond to 10% of the initial perpendicular field. In real space, this would roughly correspond to the formation of a potential structure of a few kV (for wavelength ~1000 km and perpendicular electric field ~100 mV/m). Significant parallel fields are also observed as early as at t=160. In both cases, clear effects of particle acceleration are detected in the distribution functions.

This is presented in the second panels of Figure 1 where the electron phase space density (z, V_z) is shown. The phase space density has been calculated by collecting the coordinates of all the particles present in one of the regions of density gradient (here, the region of negative gradient). For a given z, we have thus averaged the distribution function over the width of the region of density gradient. At t=160, one observes a modest bulk acceleration ($v_z \sim \pm 0.2$ at maximum) that occurs in regions of parallel electric field. The observed deformation of the distribution function is simple to follow. The maximum positive bulk velocity is observed around z=30. This more or less corresponds to the trailing edge of the region of negative parallel field (from z=30

to z=100) observed in the negative gradient region (note again that the perturbation propagates towards right). Since the Alfvén wave propagates faster than the thermal velocity, the trailing edge of the region of negative field is the region where the particles, in average, gain the maximum energy. There, the particles have indeed spent the longest time in the acceleration region.

At t=320, the bulk acceleration is still observable with roughly the same amplitude, but a halo of suprathermal particles with positive velocities is created (with $v_z = 0.3 = 3v_{te}$). To make this new population more visible in the plot, we subtract to the observed distribution function the initial thermal distribution (the same procedure is applied for figures 4 and 6). The maximum energy is observed close to $z \simeq$90. This again corresponds to the trailing edge of the region of negative field (from z=90 to z=160). In some respects, this halo presents some of the characteristics of a particle beam since it begins to be disconnected from the thermal population. We do not see a halo of such energetic particle with a negative velocity. This dissymmetry has to be related to the direction of propagation of the perturbation. In regions of negative $E_{\|}$, the electrons get a positive acceleration and will spend more time in the acceleration region. They will thus gain more energy than the ones accelerated in the opposite direction of the wave (in regions of positive $E_{\|}$).

The ion population (not shown) also undergoes a weak bulk acceleration, however, we do not see any indication for the formation of ion beams, or any significant ion heating. The only visible effect is a modulation of the density, on the scale of the incoming wave. It reaches its higher amplitude in the low density region where it is of the order of 20%.

In conclusion, the linear evolution of an Alfvén wave propagating in a density channel leads to the formation of parallel electric fields that are sufficiently strong to significantly affect the particle distribution functions (particle beam formation, in particular). This spontaneous formation of particle beams by the Alfvén wave

acceleration process is one of the important new points of the present simulation. It constitutes a first indication for the possibility of a further nonlinear evolution of the system. This will be described in the next section.

4. Non-linear evolution of the system

4.1. Creation of field aligned electron beams: development of an electrostatic instability

By comparing the second panel of Figure 3 and Figure 4 (t =480), one clearly sees that the acceleration process has increased the number of energetic particles. Many particles of the halo observed at t =320 have now velocity larger than 0.3. In the region $150 < z < 180$, a population of energetic particle is disconnected from the thermal population and thus forms a well defined beam. In fact, this stage of the evolution corresponds to the maximum particle acceleration observed during the simulation. These particles leave the acceleration region by the leading edge of the $E_{\|} < 0$ region and have gained the maximum possible energy. These runaway electrons create an electron beam downstream of the acceleration region. Considering the two gradients, one can estimate that the beams (defined as the populations of suprathermal electrons with velocity larger than 0.4) develop over a total distance that covers nearly half of the length of the simulation box.

Since particle beams propagating in plasma generate various type of small-scale producing instabilities ([*Mottez,* 2001] and references therein), it is not surprising to observe that the parallel electric field (in upper panel) now presents evidences for a short wavelength structuration. This structuration is also visible in the perpendicular E_x component and on the electron density (not shown here). In contrast, there is no similar signature on the ion density, the magnetic field or the E_y electric components. These structures (created by the beam plasma instability) are therefore electrostatic.

They appear around t =400, for $100 < z < 130$ (region of negative gradient). At t =480, they are seen for $150 < z < 180$. The instability thus follows the propagation of the Alfvén wave and is clearly associated to the region where the most energetic beam is observed.

The instability process seen here can be related to the classical evolution of a beam-plasma interaction (although we are dealing with an inhomogeneous plasma). With respect to the initial conditions of the simulation (linear propagation of the Alfvén wave in a density channel), it is a nonlinear evolution that involves the progressive generation of a parallel electric field, an efficient particle acceleration and the formation of beams. This nonlinear wave-particle coupling transfers energy from the long wavelength/low frequency domain to the short wavelength/high frequency one. This coupling between phenomena of different scales is one of the key process of the auroral particle acceleration mechanism.

4.2. Small scale structuration of the parallel electric field

To follow the non-linear development of small scale electric field structures, we present in Figure 5 the spatio/temporal evolution of the parallel electric field. The plotted quantity is an average of the parallel field over the region of negative gradient (the lower one on previous figures). The z direction is in abscissa and the time is in ordinates. To facilitate the analysis and to simplify the study of the propagation of some particular structures, we have duplicated the periodic box of simulation in the space direction (z extends now to $409.6c/\omega_{pe}$).

This figure shows the very fast and strong modification of the morphology of the electric field that occurs from t=400 to t=500. Before t=350, one observes the linear Alfv/'en wave propagation described in section 3. A long wavelength parallel electric field with a typical scale of the order of the wavelength of the initial Alfvén wave propagates at the Alfvén velocity. Its amplitude progressively increases and reaches

0.002 at t=350. From Figures 3 and 4, we already know that this stage of the evolution corresponds to the formation of an electron beam. Around t=350, a first type of small scale modifications of the electric field is observed. It corresponds to waves which propagate slowly backwards (toward $z < 0$, $v \simeq -0.05$). Their amplitude remain modest (less than 0.005) and they decay rapidly. A more detailed analysis (a Fourier transform in both space and time, and a fit to dispersion relations) suggests that they may be ion-acoustic waves. The condition $T_e \gg T_i$, mandatory for the ion-acoustic instability, is indeed satisfied at this time. These modulations are marginal compared to the strong fluctuations of larger scale which begin to be observable around t=450. These large structures are generated by the beam-plasma instability. They appear in the region of negative electric field where the electron beam is particularly well defined. They propagate in the positive direction at a velocity close to the Alfvén one and largely dominates the organization of the electric field from t=450 to t=1000 (their electric amplitude is as high as 0.02 which is also the initial $E_\perp$ amplitude).

One notes that a structuration of the electric field is also seen in the positive electric field region. This structuration does not correspond to a direct local beam/plasma instability. Indeed, with the range of parameters used here, we do not observed electron beams with $v_z < 0$. The observed structuration in this region is in fact an effect of the perpendicular extension of the small scale structures from the positive gradient region. The structures indeed extend further than the density gradient into the cavity and finally reach the opposite gradient. For example, at t=480 around $70 < z < 90$ on Figure 4, the structured parallel field from the positive gradient reaches the negative gradient.

To understand the sign of the parallel electric field, we refer to [*Génot et al.,* 1999] where it is shown that, in first approximation, $E_\parallel \propto E_\perp / n.\partial n/\partial x$; this means that the parallel electric field is of the same sign as the incoming perpendicular electric field on the positive density gradient. Therefore, for a given altitude z the parallel fields created

in the two gradient regions are of opposite sign.

The typical spatial scale of the structures is $\Delta_z \sim 3 - 10c/\omega_{pe} \sim 30 - 100\lambda_D$ (with a mean $\sim 7c/\omega_{pe}$) and their typical electric amplitude is $E_z \sim \pm 0.015$. This corresponds to an associated potential difference along the magnetic field direction of: $\Phi \simeq E_z \Delta_z \sim 0.1 m_e c^2/e$. This is 10 times greater than the initial thermal electron energy. The structures are roughly separated from each other by a typical distance of $10c/\omega_{pe} = 100\lambda_D$ and they can be considered as stable since they can last for more than $400\omega_{pe}^{-1}$.

Some interesting points concerning their spatio-temporal development are worth to be noticed. When they appear (for $400 < t < 500$), they simply correspond to a small scale structuration of the pre-existing parallel electric field. In particular, their associated field has the same sign as the large scale parallel field. However, the amplitude of these structures progressively increases and, at t=600, reversal in the parallel electric field begin to be observable: the electric field is then bipolar. These strong structures presenting a reversal of the electric field are observable until t=900. They exist in a region with a typical 50 c/ω_{pe} extension (for example, $200 < z < 250$ at t=700). It is in this region that the particles of largest energies are observed. This corresponds to the transition between a region of negative field (region of acceleration in the sense of the Alfvén wave propagation) and a region of positive field. Elsewhere, in the main part of the region of positive acceleration and in the leading edge of the region of negative acceleration, structures of smaller amplitude are observed. They are not associated to a reversal of the electric field and a net potential difference exists between their two sides. In other words, we observed two types of non linear structures. The largest ones, with reversal of the electric field, can be considered as the classical non-linear structures already described in numerous studies of the nonlinear evolution of the beam-plasma instability. The smaller other ones can be described as weak double layer. They indeed present a net potential difference between their two sides. After

t=900, the amplitude of the structures progressively decreases and for $t > 1000$, one can consider that the signature of the nonlinear process is strongly reduced. The simulation stops at t=1200. At that time, parallel electric fields of constant direction, but still presenting traces of structuration, exist over spatial scales of the order of the Alfvén wavelength.

Apart from a few slower structures on the trailing edge of the negative electric field region, most of them initially propagate at the Alfvén velocity. They are subsequently accelerated, up to $v \simeq 0.6$ for the fastest ones. The acceleration is seen on Figure 5 as a curvature of initially straight lines (for instance around z=255 at t=640). These structures are supported by the most energetic electrons, their dispersion relation can be expressed as $\omega/k \simeq v_{ES}$ with $0.27 < v_{ES} < 0.6$, (v_{ES} being the beam velocity). These fast structures finally reach the positive electric field region where they disappear (for example, at z=800 for t=700).

We finally note that these non linear signatures have an amplitude that increases with their spatial length. This behaviour is opposite to the one of the acoustic Korteg-de Vries solitons but is similar to the one of electric structures associated with electron holes.

4.3. Bi-dimensional structure: phase space analysis

Using the same type of plot than for Figures 2, 3 and 4, we present in Figure 6 a map of the parallel electric field and of the electron phase space density during the late phase of the non-linear evolution (t=800).

A first interesting point concerns the bi-dimensional extension of the non-linear structures. They are indeed much wider than the regions of gradient where the maximum acceleration is expected. This effect is already visible in Figure 4 and corresponds to the fact that the region of formation of the beam fills almost the whole density channel. We have still not identified the process at work for the widening of the structures and

further studies will be needed to clarify this point. The subsequent evolution of the structures also shows a loss of coherence in the perpendicular dimension: they become divided. Two recent simulation studies on this subject suggest that oblique waves are responsible for this striation when ion dynamics is retained. Depending on the plasma regime (basically the electron cyclotron to plasma frequency ratio), [*Goldman et al.,* 1999] found that whistler waves are involved, whereas [*Miyake et al.,* 2000] found lower hybrid waves. Our simulations is closer to the first study. This nevertheless suggests that, if the density gradients have to be considered as the initial site where the Alfvén waves acquire a parallel field, the region concerned by the energy conversion process could be much wider (the whole density cavity).

A second point concerns the effect of the non-linear structures on the distribution functions. They strongly modulate both the particle beam and the thermal distribution function. For example at t=800, the strong structure seen at z=90 is associated to a global shift of the bulk velocity. Over a short scale ($88 < z < 92$), this velocity indeed becomes negative (around $-v_{te}$) which indicates that a strong energy exchange locally takes place. The electron population reacts as a whole to the formation of the non-linear structure. This structure presents some differences with the electron holes seen by FAST [*Ergun et al.,* 1998b], and analytically studied by [*Muschietti et al.,* 1999], since it does not correspond to a hole in the distribution function that would be described as a BGK mode. It is nevertheless possible to identify around $z = 60$ two structures that may present some similarities with electron holes. They were already present at t=640 for $z = 60$. They are observed in a region where the beam is not completely disconnected from the thermal distribution. In this region of the phase space, the electric structures create a hole in the distribution function (high energy population and lack of middle energy population) by particle trapping. Nevertheless, at the difference with the FAST observations, these holes are not centered at $v = 0$.

5. Discussion and conclusion

Given the specificity of the regime of parameters used in the simulation (in particular, the unrealistic electron/ion mass ratio), the comparison between our results and spacecraft observations is not straightforward. We nevertheless obtain a series of new results that could help to understand the auroral acceleration mechanism. For the first time, we self-consistently simulate the chain of processes that could connect the formation of parallel electric field on large scales and the non-linear evolution towards smaller scales. These processes also couple the formation of HF electrostatic structures to LF electromagnetic waves. We focus on a very general system which consists in the interaction of an incoming Alfvén wave with a plasma cavity (inhomogeneity in the transverse direction). The evolution of this system is studied and leads to the following consequences:

- During an initial phase, a parallel electric field is created in the gradient regions, in both directions and on the scale of the incoming wavelength.
- Due to the direction of propagation of the incoming Alfvén wave, a dissymmetry appears in the energy exchange with the electron population. The maximum acceleration occurs in regions where the parallel electric field is opposite to the direction of the incoming wave propagation.
- As a result of this acceleration, runaway electrons escape from the region where they have been initially accelerated and create a beam, downward the acceleration region. In our simulation, this corresponds to the region of negative field.
- This beam is unstable. An electrostatic instability takes place which leads to a fast short scale structuration of the parallel electric field.
- Different types of nonlinear structures form. Some of them keep a modest amplitude, they do not present a reversal of the electric field and can be

assimilated to weak double layers. Stronger ones, associated to reversal of the field, are also observed and present similarities with electron phase holes.

We also note that the whole process takes place in a region much wider than the initial density gradients since the whole density channel is strongly affected by the nonlinear evolution. Even if new studies are needed to better understand the observed processes, the simulations presented here constitute a first step in the description of the coupling between low frequency electromagnetic phenomena and the short scale structuration of the accelerating electric field. They also confirm that the low frequency phenomena are potentially important for the auroral acceleration.

Acknowledgments. VG is supported by a UK PPARC grant. The numerical computations have been supported by IDRIS (CNRS computation center, France).

References

Alfvén, H., and C.G. Fälthammar, Cosmical Electrodynamics, pp. 163-167, Clarendon, Oxford, 1963.

Bellan, P. M., and K. Stasiewicz, Fine-scale cavitation of ionospheric plasma caused by inertial Alfvén wave ponderomotive force, *Phys. Rev. Lett., 80,* 3523, 1998.

Berthomier, M., R. Pottelette, and M. Malingre, Solitary waves and weak double layers in a two-electron temperature auroral plasma, *J. Geophys. Res., 103*, 4461, 1998.

Bingham, R., D. A. Bryant, and D. S. Hall, A wave model for the aurora, Geophys. Res. Lett., 11, 327, 1984.

Boström, R., G. Gustafsson, B. Holback, G. Holmgreen, H. Koskinen, and P. Kintner, Characteristics of solitary waves and weak double layers in the magnetospheric plasma, *Phys. Rev. Lett., 61*(1), 82, 1988.

Chaston, C. C., C. W. Carlson, W. J. Peria, R. E. Ergun, and J. P. McFadden, Fast observations of inertial Alfvén waves in the dayside aurora, *Geophys. Res. Lett., 26,*, 647, 1999.

Chiu Y. T. and M. Schulz, Self-consistent particle and parallel electrostatic field distributions in the magnetospheric-ionospheric auroral region, *J. Geophys. Res., 83,* 629, 1978.

Chmyrev et al., Non-linear Alfvn wave generator of auroral particles and ELF/VLF waves, Planet. Spac. Sci., 37, 749, 1989.

Chust, T., P. Louarn, M. Volwerk, H. de Feraudy, A. Roux, J. Wahlund, and B. Holback, Electric fields with a large parallel component observed by the FREJA spacecraft: Artifacts or real signals ?, *J. Geophys. Res., 103,* 215, 1998.

Clark, A. E., and C. E. Seyler, Electron beam formation by small-scale oblique inertial Alfvén waves, *J. Geophys. Res., 104,* 17233, 1999.

Ergun, R. E., C. W. Carlson, J. P. McFadden, F. S. Mozer, G. T. Delory, W. Peria, C. C. Chaston, M. Temerin, R. Elphic, R. Strangeway, R. Pfaff, C. A. Cattell, D. Klumpar,

E. Shelley, W. Peterson, E. Moebius, and L. Kistler, FAST satellite observations of electric field structures in the auroral zone, *Geophys. Res. Lett., 25,*, 2025, 1998.

Ergun, R. E., C. W. Carlson, J. P. McFadden, F. S. Mozer, G. T. Delory, W. Peria, C. Chaston, M. Temerin, I. Roth, L. Muschietti, R. C. Elphic, R. Strangeway, R. Pfaff, C. A. Cattel, D. Klumpar, E. Shelley, W. Peterson, E. Moebius, and L. Kistler, FAST satellite observations of large-amplitude solitary structures, *Geophys. Res. Lett., 25,*, 2041, 1998.

Génot, V., P. Louarn, and D. Le Quéau, A study of the propagation of Alfvén waves in the auroral density cavities, *J. Geophys. Res., 104,* 22,649, 1999.

Génot, V., F. Mottez, and P. Louarn, Electron acceleration by Alfvén waves in density cavities, *J. Geophys. Res., 105,* 27,611, 2000.

Génot, V., F. Mottez, and P. Louarn, Particle acceleration linked to Alfvén wave propagation on small scale density gradients, *J. Phys. and Chem. of the Earth, Part C*, 26, 2001, Proc. 2nd EGS Alfvén conference on particle acceleration, Stockholm, May 1999.

Goertz, C. K., and R. W. Boswell, Magnetosphere-ionosphere coupling, *J. Geophys. Res., 84,* 7239, 1979.

Goldman, M. V., M. M. Oppenheim, and D. L. Newman, Nonlinear two-stream instabilities as an explanation for auroral bipolar wave structures, *Geophys. Res. Lett., 26,* 1821, 1999.

Hasegawa, A., Particle acceleration by MHD surface wave and formation of aurora, *J. Geophys. Res., 81,* 6083, 1976.

Kletzing, C. A., Electron acceleration by kinetic Alfvén waves, *J. Geophys. Res., 99,* 11095, 1994.

Knudsen, D. J., Spatial modulation of electron energy and density by nonlinear stationary inertial Alfvén waves, *J. Geophys. Res., 101,* 10761, 1996.

Louarn, P., J. E. Wahlund, T. Chust, H. de Feraudy, A. Roux, B. Holback, P. O. Dovner, A. I. Eriksson, and G. Holmgren, Observation of kinetic Alfvén waves by the FREJA spacecraft, *Geophys. Res. Lett., 21,* 17, 1994.

Lysak, R. L., and C. T. Dum, Dynamics of magnetosphere-ionosphere coupling including turbulent transport, *J. Geophys. Res., 88,* 365, 1983.

Lysak, R. L., Electrodynamic coupling of the magnetosphere and ionosphere, *Space Sci. Rev., 52,* 33, 1990.

Lysak, R. L., and W. Lotko, On the kinetic dispersion relation for shear Alfvén waves, *J. Geophys. Res., 101,* 5085, 1996.

Mandrake, L., P. L. Pritchett, and F. V. Coroniti, Electron beam generated solitary structures in a nonuniform plasma system, *Geophys. Res. Lett., 27,* 2869, 2000.

Mälkki, A., A.I. Eriksson, P.O. Dovner, R. Boström, B. Holback, G. Holmgren, and H.E.J. Koskinen, A statistical survey of auroral solitary waves and weak double layers, Occurence and net voltage, *J. Geophys. Res., 98*, 15,521, 1993.

Mangeney, A., C. Salem, C. Lacombe, J.-L. Bougeret, C. Perche, R. Manning, P. J. Kellogg, K. Goetz, S. J. Monson, and J.-M. Bosqued, WIND observations of coherent electrostatic waves in the solar wind, *Ann. Geophysicae., 17*, 307-320, 1999.

Miyake, T., Y. Omura, and H. Matsumoto, Electrostatic particle simulations of solitary waves in the auroral region, *J. Geophys. Res., 105*, 23,239, 2000.

Mottez, F., G. Chanteur, and A. Roux, Filamentation of plasma in the auroral region by an ion-ion instability: A process for the formation of bidimensional potential structures, *J. Geophys. Res., 97*, 10,801, 1992.

Mottez, F., S. Perraut, A. Roux, and P. Louarn, Coherent structures in the magnetotail triggered by counterstreaming electron beams *J. Geophys. Res., 102*, 11,399, 1997.

Mottez, F., J.C. Adam and A. Heron, A new guiding centre PIC scheme for electromagnetic highly magnetized plasma simulation, *Computer Physics Communication 113*, pp 1-22, 1998.

Mottez, F., Instabilities and Formation of Coherent Structures, to be published in *Astrophys. Space Sci.*, special issue, proceedings of the conference OBS2000, Meudon, France, 2001.

Miura, A and T. Sato, numerical simulation of global formation of auroral arcs, *J. Geophys. Res., 85,* 73, 1980.

Muschietti, L., R. E. Ergun, I. Roth, C. W. Carlson, Phase-space electron holes along magnetic field lines, *Geophys. Res. Lett., 26*, 1093, 1999

Omura, Y., H. Matsumoto, T. Miyake, and H. Kojima, Electron beam instabilities as generation mechanism of electrostatic solitary waves in the magnetotail, *J. Geophys. Res., 101*, 2685, 1996.

Papadopoulos, K., A review of anomalous resistivity for the ionosphere, Rev. Geophys. Spac. Res., 15, 113, 1977.

Seyler, C. E., A mathematical model of the structure and evolution of small-scale discrete auroral arcs, *J. Geophys. Res., 95,* 17199, 1990.

Seyler, C. E., J. E. Wahlund, and B. Holback, Theory and simulation of low-frequency plasma waves and comparison to Freja satellite observations, *J. Geophys. Res., 100,* 21453, 1995.

Seyler, C. E., and J.-E Wahlund, Theory of nearly perpendicular electrostatic plasma waves and comparison to Freja satellite observations, *J. Geophys. Res., 101,* 21795, 1996.

Stasiewicz, K., G. Holmgren, L. Zanetti, Density depletions and current singularities observed by Freja, *J. Geophys. Res., 103,* 4251, 1998.

Streltsov, A. V., and W. Lotko, Dispersive field line resonances on auroral field lines, *J. Geophys. Res., 100,* 19457, 1995.

Streltsov, A. V., Dispersive width of the Alfvénic field line resonance, *J. Geophys. Res., 104,* 22657, 1999.

Temerin, M., C. A. Catell, K. Cerny, W. Lotko and F. S. Mozer, Observations of double layers and solitary waves in auroral plasma, Phys. Rev. Lett., 48, 164, 1982.

Volwerk, M., P. Louarn, T. Chust, A. Roux, H. de Féraudy, and B. Holback, Solitary kinetic Alfvén waves: A study of the Poynting flux, *J. Geophys. Res., 101,* 13335, 1996.

Wahlund, J. E., Louarn, P., T. Chust, H. de Féraudy, A. Roux, B. Holback, P.O. Dovner, and G. Holmgren, On ion-acoustic turbulence and the nonlinear evolution of kinetic Alfvén waves, *Geophys. Res. Lett., 21,* 1831, 1994.

V. Génot, Astronomy Unit, Queen Mary, University of London, Mile End Road, London E1 4NS, England, UK. (v.genot@qmw.ac.uk)

P. Louarn, Centre d'Etude Spatiale des Rayonnements, 9 Av. Colonel Roche, 31400 Toulouse, France. (louarn@cesr.fr)

F. Mottez, Centre d'étude des Environnements Terrestre et Planétaires, 10-12 Av. de l'Europe, 78140 Vélizy, France. (fabrice.mottez@cetp.ipsl.fr)

Received _____

For submission to *J. Geophys. Res.*

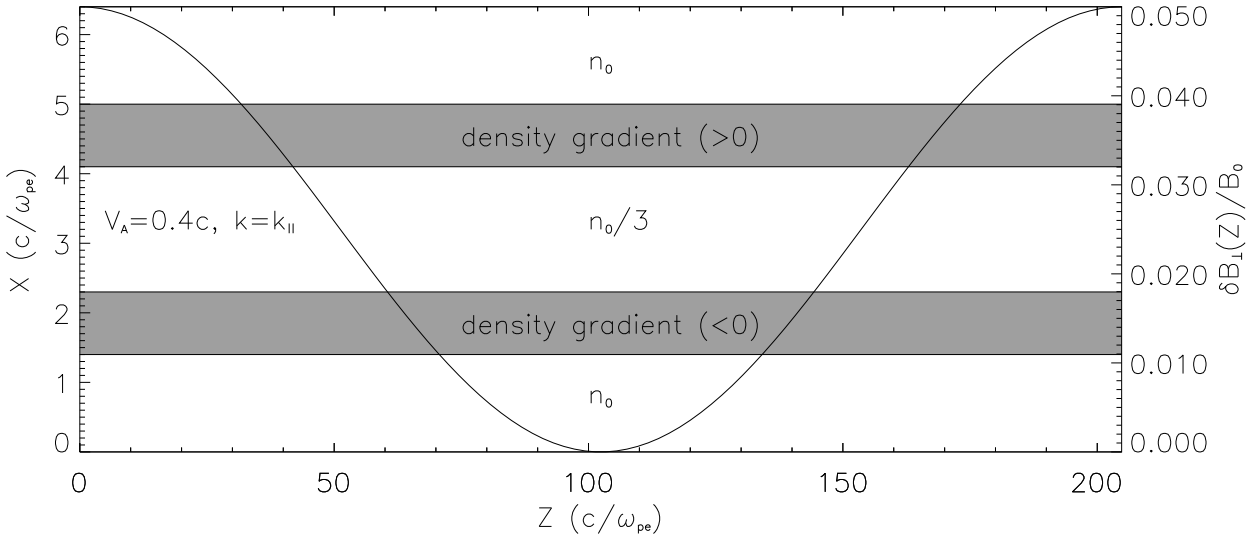

Figure 1. Initial configuration of the simulation box. The density cavity is presented as a channel (depletion in the center). The Alfvén wavelength is equal to the parallel size ($204.8c/omega_{pe}$).

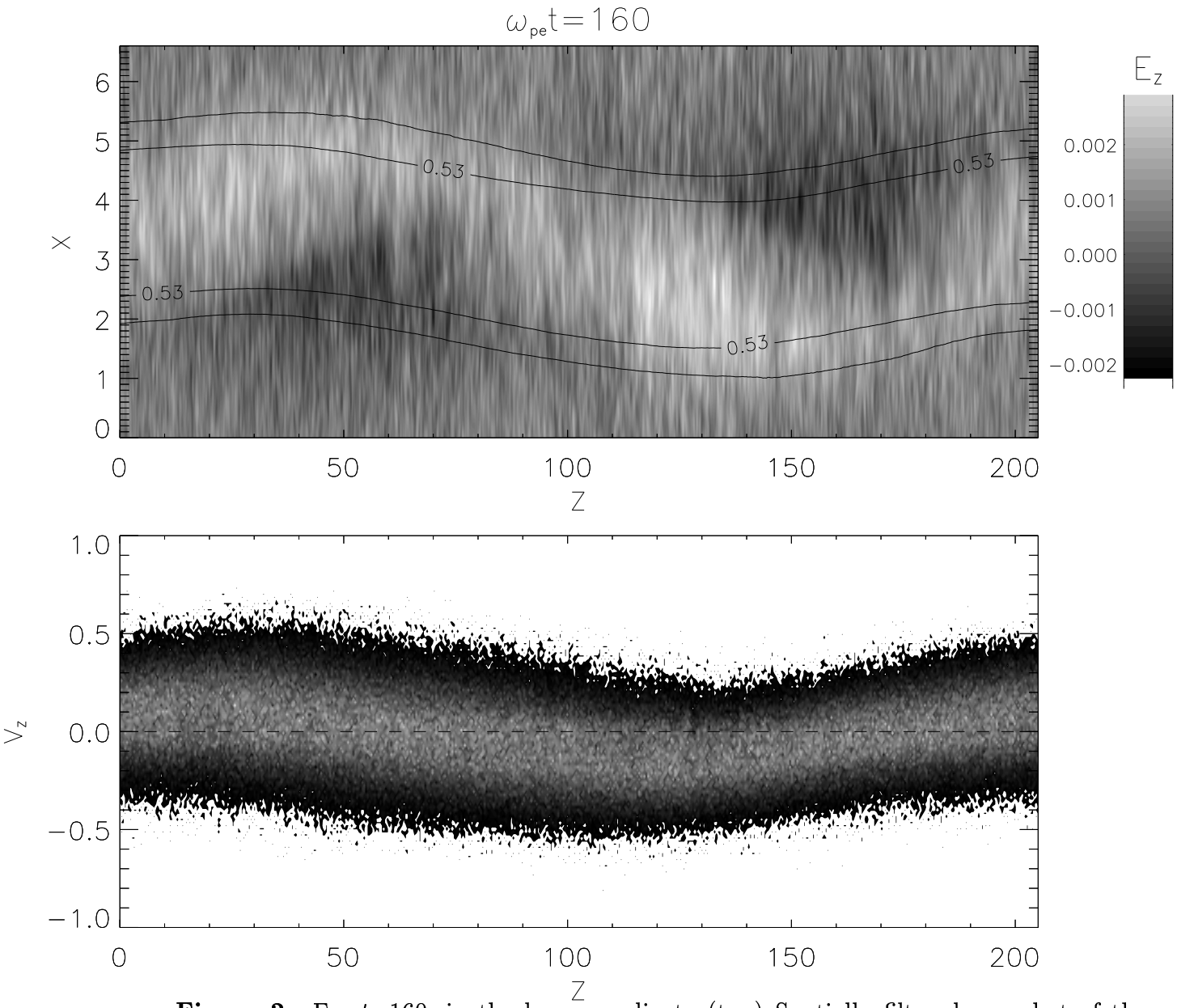

Figure 2. For t=160, in the lower gradient: (top) Spatially filtered snapshot of the parallel electric field $E_z(z,x)$ with superimposed electron density contours (bounding the gradient regions). (bottom) Electron phase space (z, v_z).

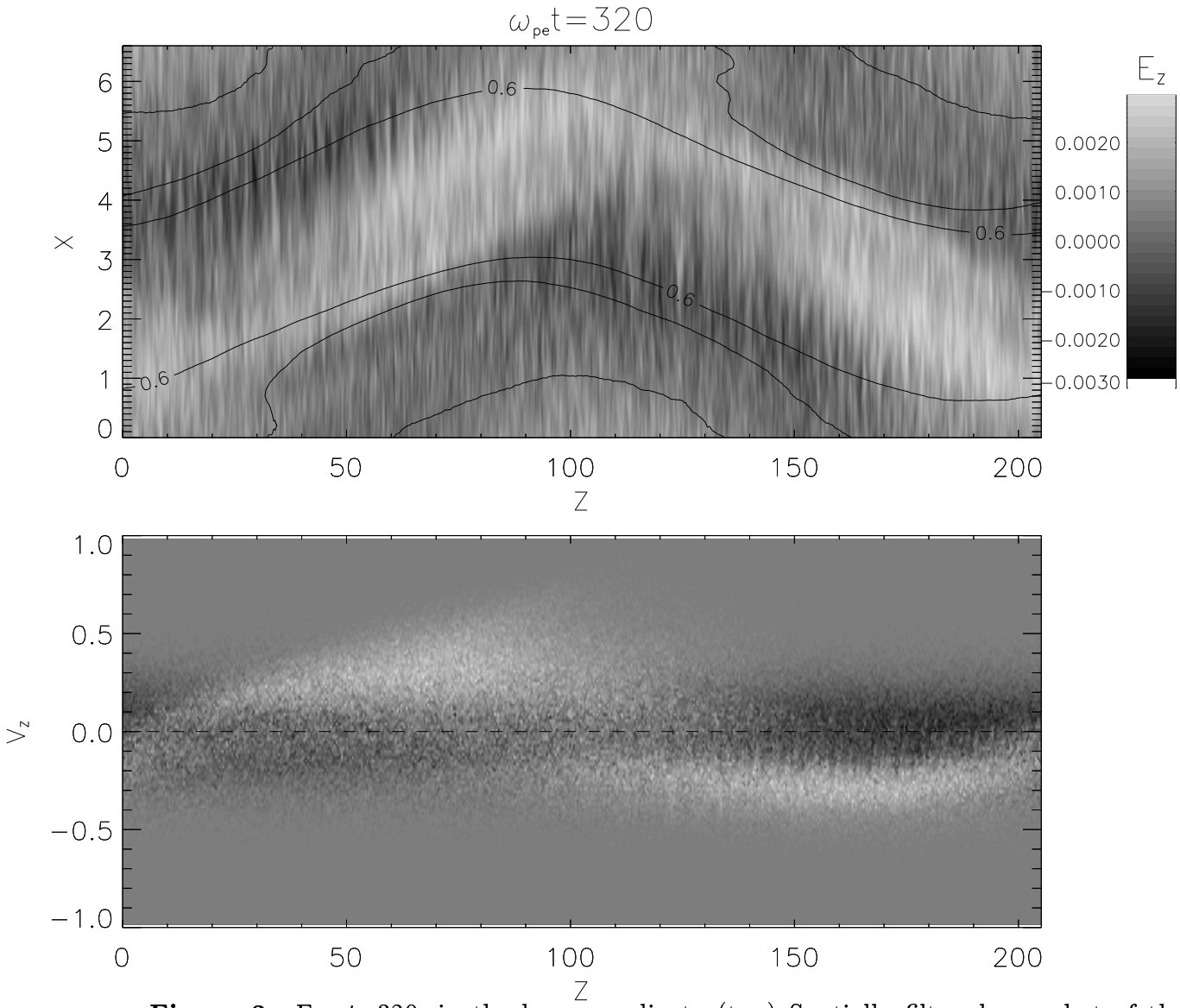

Figure 3. For t=320, in the lower gradient: (top) Spatially filtered snapshot of the parallel electric field $E_z(z,x)$ with superimposed electron density contours (bounding the gradient regions). (bottom) Differential electron phase space (z, v_z): the initial thermal distribution (Gaussian) function has been subtracted.

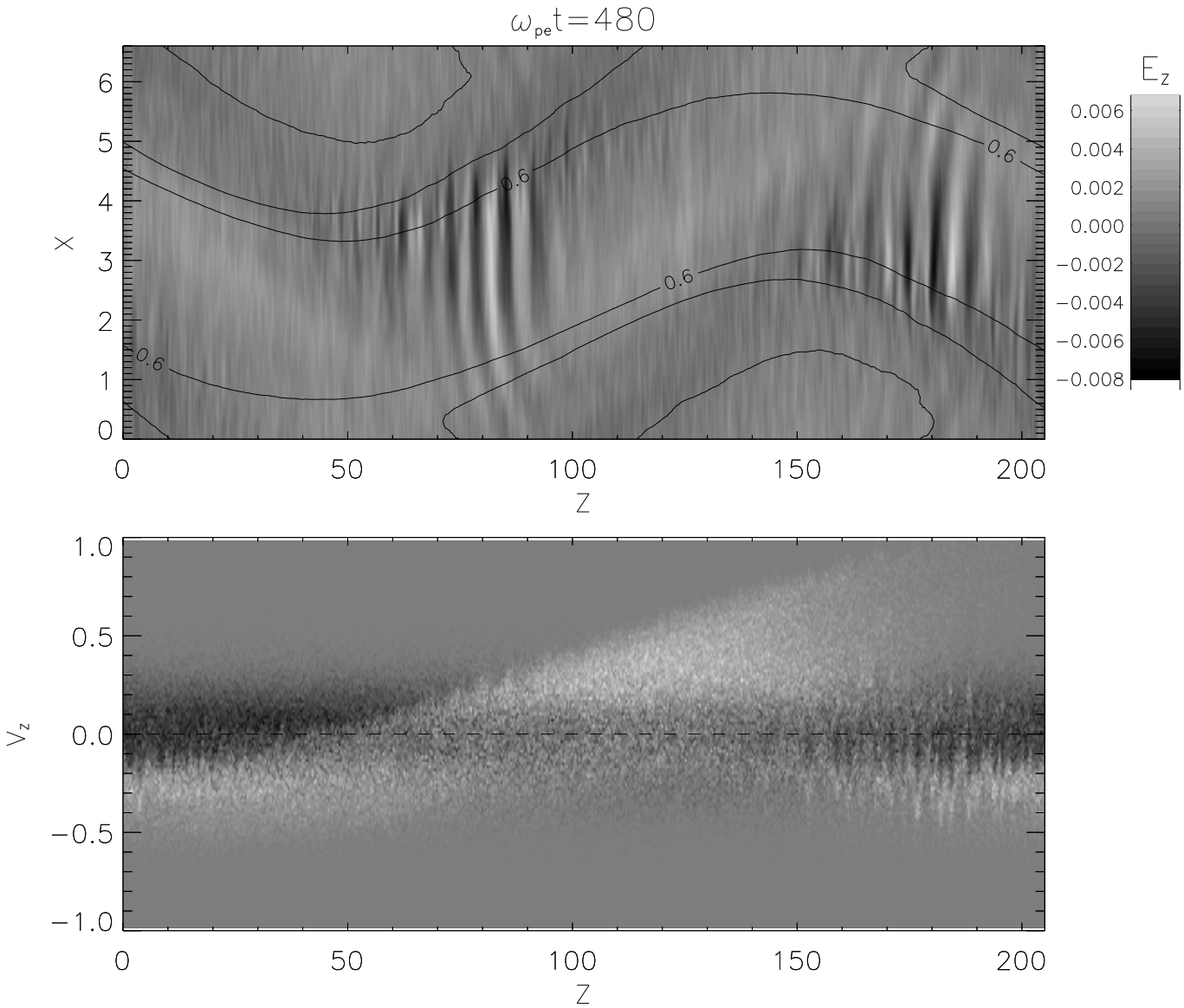

Figure 4. Same as Figure 3 for t=480

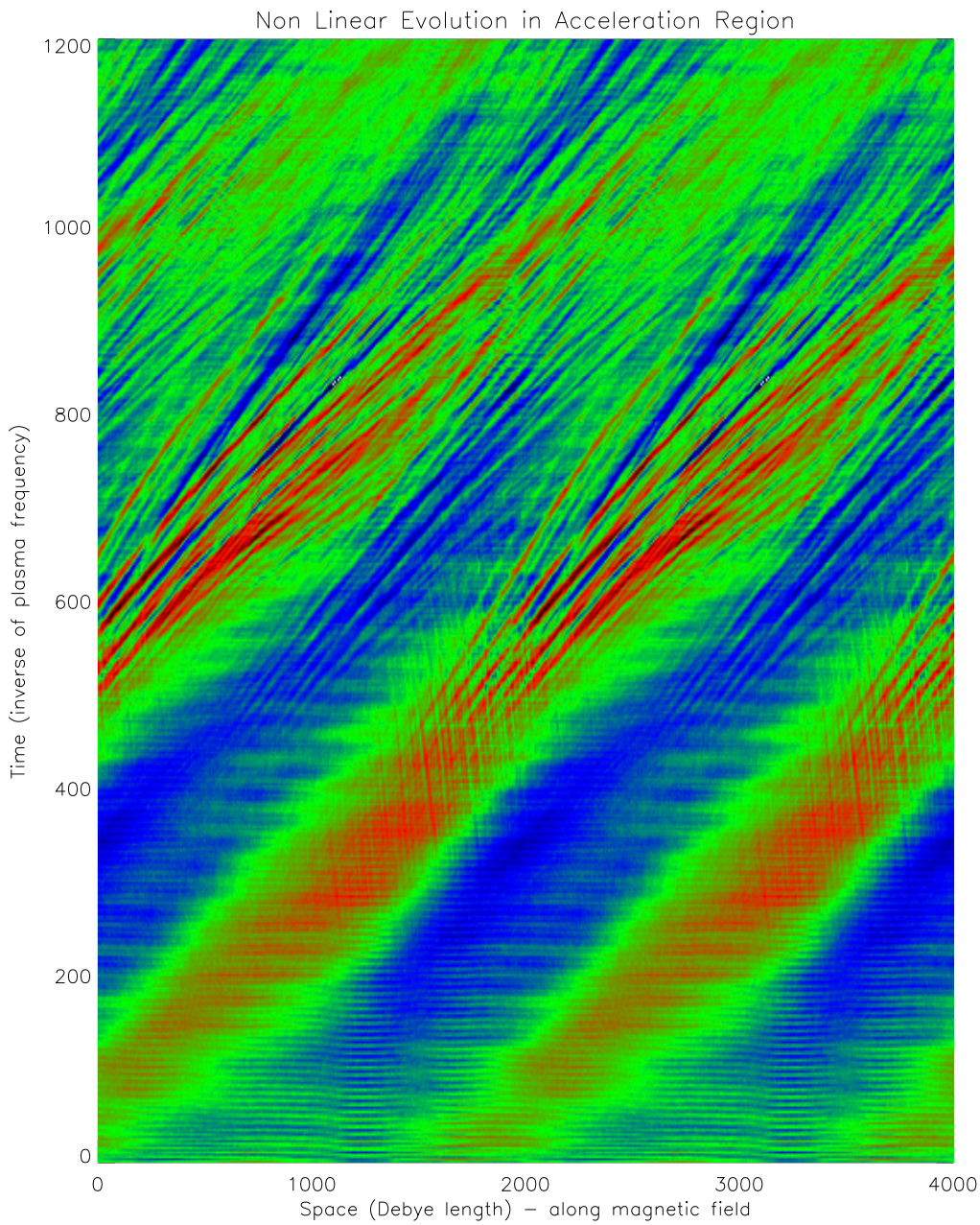

Figure 5. The parallel electric field E_z as a function of z and t integrated over the lower density gradient boundaries. The spatial extension has been doubled by using periodic conditions.

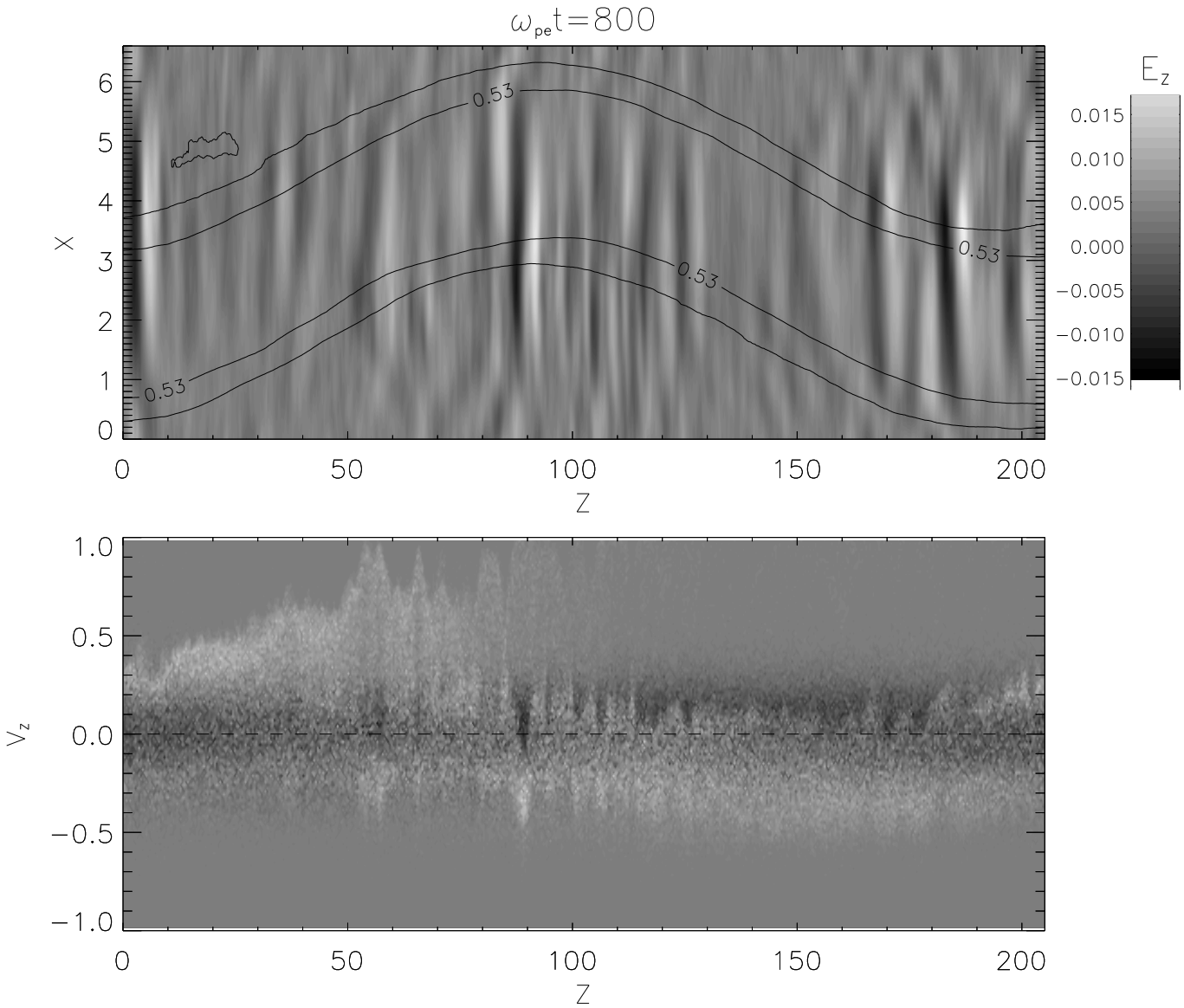

Figure 6. Same as Figure 3 for t=800.